BIOCHEMISTRY
including biophysical chemistry & molecular biology

Article

pubs.acs.org/biochemistry

Effect of Dimerization on Dihydrofolate Reductase Catalysis

Jiannan Guo, E. Joel Loveridge, Louis Y. P. Luk, and Rudolf K. Allemann*

School of Chemistry and Cardiff Catalysis Institute, Cardiff University, Main Building, Park Place, Cardiff CF10 3AT, United Kingdom

Supporting Information

ABSTRACT: Dihydrofolate reductase (DHFR) from the hyperthermophile *Thermotoga maritima* (TmDHFR) forms a very stable homodimer, while DHFRs from other organisms are monomers. We investigated the effect of dimerization on DHFR catalysis by preparing a dimeric variant, Xet-3, of DHFR from *Escherichia coli* (EcDHFR). Introducing residues located at the TmDHFR dimer interface into EcDHFR increases the melting temperature to ∼60 °C, approximately 9 °C higher than that measured for EcDHFR. The steady-state and pre-steady-state rate constants measured for Xet-3 were similar to those of dimeric TmDHFR but significantly lower than those of the parent EcDHFR. This reduction in the degree of catalytic competence is likely a consequence of the loss of flexibility of catalytically important loop regions of EcDHFR on dimerization and a compromise of the electrostatic environment of the active site. In contrast, the reduced catalytic ability of TmDHFR relative to that of EcDHFR is not simply a consequence of reduced loop flexibility in the dimeric enzyme. Our studies demonstrate that EcDHFR is not a good model for understanding the properties of other DHFRs, including TmDHFR.

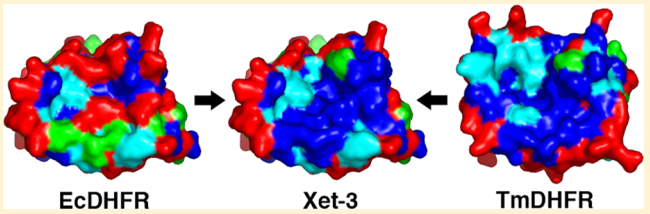

Thermophiles grow optimally at ≥50 °C[1] and offer great potential for industrial uses. Comparative studies between thermophilic and mesophilic enzymes have revealed that greater hydrophobicity,[2] better atom packing,[3] introduction of proline residues into loops,[2,4,5] increased levels of hydrogen bonding,[6,7] increased levels of ionic bonding,[2,3] and oligomerization[8] can work together to enhance the thermal stability of proteins. These stabilizing interactions create more rigid conformations, which stabilize the folds of thermophilic proteins. Their effects on catalysis are, however, less well understood, and the relationship between conformational flexibility and catalysis is still a matter of considerable debate.[9−12] It has been argued that the reduced catalytic power of thermophilic enzymes at a given temperature is a consequence of the reduced flexibility of thermophilic enzymes.[13−15] Although comparisons of homologous enzymes isolated from organisms from different thermal niches are useful, more detailed studies are needed to establish a complete understanding of how thermophilic enzymes remain active over a wide temperature range.

The monomeric enzyme dihydrofolate reductase from the mesophile *Escherichia coli* (EcDHFR), an essential catalyst for the NADPH-dependent reduction of 7,8-dihydrofolate (H_2F) to 5,6,7,8-tetrahydrofolate (H_4F),[16,17] is a popular model in the study of biophysical properties of enzymes, including thermal adaptation, and EcDHFR has been coined a paradigm for enzyme catalysis.[18] EcDHFR and the enzyme from the hyperthermophile *Thermotoga maritima* (TmDHFR) have 25% identical sequences and possess similar tertiary structures, but their thermostabilities are significantly different. With a thermal melting temperature (T_m) of 83 °C,[19] TmDHFR is indeed the most thermostable DHFR among all that have been characterized to date.[20−22] However, the catalytic activity of TmDHFR is relatively poor, and the turnover number (k_{cat}) is 10−100-fold lower than that of EcDHFR over the entire accessible temperature range.[19]

Interestingly, similar to some other enzymes from *T. maritima*, such as exopolygalacturonase, which forms a unique tetramer in solution,[23] TmDHFR is the only chromosomally encoded DHFR known to form a stable homodimer (it is likely that DHFRs from other *Thermotoga* species also form dimers, but none have yet been characterized[24]). Dimerization contributes significantly to the enhanced thermal stability of TmDHFR.[25−27] Oligomerization has been implicated as a key strategy for enhancing an enzyme's thermostability,[8] but its effect on catalysis has not been systematically elucidated. For the mesophilic EcDHFR, catalytic efficiency depends on the movement of the M20 and βFG loops.[28−30] In contrast, the corresponding loops of TmDHFR make up part of the dimer interface, forming a tightly packed hydrophobic core (Ile15, Val19, Trp22, Tyr125, and Phe127 in one subunit and Tyr140 in the other) and a key intermolecular ion pair (Lys129 of one subunit with Glu136 and Glu138 of the other).[25] These intersubunit interactions constrain free movement of the loops corresponding to the M20 and βFG loops of EcDHFR.[31]

Characterization of the kinetic properties of TmDHFR-V11D, a variant of TmDHFR that could be "switched" between the dimeric and monomeric forms by addition of the nondenaturing detergent 3-[(cholamidopropyl)-dimethyl-ammonio]-1-propanesulfonate (CHAPS), which did not

Received: April 23, 2013
Revised: May 7, 2013
Published: May 14, 2013

perturb the properties of wild-type TmDHFR, showed that the lower rate constants in TmDHFR are not simply a consequence of the restricted movements of the loops in the dimer interface.[26] Monomerization of TmDHFR-V11D had only a small effect on the rate constant for hydride transfer but reduced the rate of steady-state turnover almost 20-fold. Therefore, even when unconstrained by the dimer interface, the loop regions of TmDHFR do not seem to conduct the functions ascribed to them in the monomeric EcDHFR.[26] Instead, constraints on the position of the loops due to dimerization prevent proper closure of the active site, leading to the reduced activity of TmDHFR.[32] Here, we report the characterization of an EcDHFR variant, Xet-3, in which polar residues in the M20 loop and C-terminal sheet regions were replaced with residues involved in dimerization in TmDHFR. Our results suggest that loop flexibility is not an important factor in TmDHFR catalysis. TmDHFR is not simply a dimeric version of EcDHFR, which in turn appears not to be a good model system for DHFR catalysis.

MATERIALS AND METHODS

Chemicals. NADPH was purchased from Melford. NADPD was synthesized from $NADP^+$ (Melford) using alcohol dehydrogenase from *Thermoanaerobacter brockii* and d_8-2-propanol (Sigma-Aldrich) as described previously.[33] H_2F was prepared from folic acid (Sigma-Aldrich) and purified by repeated crystallization by the method of Zakrzewski.[34] NADPH/NADPD and H_2F concentrations were determined spectrophotometrically using extinction coefficients of 6200 cm^{-1} M^{-1} at 339 nm[35] and 28000 cm^{-1} M^{-1} at 282 nm,[36] respectively. Synthetic oligonucleotides were purchased from Eurofins MWG Operon (Ebersberg, Germany).

Xet-3 Plasmid Construction. A DNA fragment encoding the mutated C-terminal region of EcDHFR [5′-GTCATCCCGGCAGTGGTGGAAGGCGACACCCATTTCCCGGATTACGAGCCGGATGACTGGGAACTTGTATTCATGGAATTCCACGATGCTGATGCGCAGAACTCTCACGGCTATCTTTTTCTC-3′ (changes underlined)] was purchased from Epoch Biolabs. A second fragment was obtained from a pJGetit-based vector harboring the gene encoding wild-type EcDHFR, using the primers 5′-ATTCTGGAGCGGCGGTAA-3′ (forward) and 5′-CGTCAGATACAGTTTTTGCG-3′ (reverse) under standard polymerase chain reaction conditions. This second fragment consisted of the N-terminal sequence of EcDHFR and the vector. The two fragments were ligated by T4 DNA ligase to form a pJGetit-based vector harboring a gene encoding a partial EcDHFR−TmDHFR hybrid. The N-terminal mutations, D11S and R12G, were generated using the Phusion Site-Directed Mutagenesis Kit (New England Biolabs) following the manufacturer's instructions. The mutagenic primers were 5′-GCGTTAGCGGTATCTCGCGTTATCGG-3′ and 5′-GTTAGCGGTATCTGGCGTTATCGGCATG-3′ (changes underlined). The final product was excised from the pJGetit-based vector and subcloned into pET11c at restriction sites *Nde*I (5′) and *Bam*HI (3′). The sequence of Xet-3 DNA was verified by automated DNA sequencing (Molecular Biology Unit, Cardiff University).

Protein Purification. *E. coli* BL21(DE3) cells were transformed with the plasmid carrying the Xet-3 DNA and grown in LB medium containing ampicillin (100 μg/mL) to an OD_{600} of 0.6. Isopropyl β-D-thiogalactopyranoside (Melfold) was added to a final concentration of 1 mM. Cells were grown overnight at 30 °C and harvested by centrifugation. A significant portion of the protein was found in inclusion bodies. The pellet from a 0.5 L cell culture was resuspended in 30 mL of potassium phosphate buffer (50 mM, pH 7) and disrupted by sonication. The supernatant was decanted and the pellet washed with 30 mL of 1% Triton X-100, followed by 30 mL of 2 M urea. Inclusion bodies were dissolved in 40 mL of 8 M urea at 4 °C overnight. Insoluble proteins were removed by centrifugation. Refolding was then performed by a gradual 5-fold dilution of the denatured proteins with refolding buffer [50 mM Tris-HCl, 100 mM NaCl, and 400 mM arginine (pH 8.0)] over 6 h. Urea and arginine were removed by dialysis. The refolded proteins were applied to a DEAE-sepharose resin pre-equilibrated with 50 mM Tris-HCl (pH 8.0) and eluted with a 0 to 1 M NaCl gradient.

Size Exclusion Chromatography. Size exclusion chromatography was performed on a Superdex 75 10/300 GL column (GE Healthcare) at a flow rate of 0.5 mL/min. Enzyme concentrations of 20 μM were used in 100 mM potassium phosphate (pH 7.0) containing 100 mM NaCl.

Circular Dichroism (CD) Spectroscopy. CD spectroscopy was conducted on an Applied PhotoPhysics Chirascan spectrometer. CD spectra between 200 and 280 nm were measured for enzyme (10 μM) in degassed potassium phosphate buffer (10 mM, pH 7.0). The observed signal was converted into mean residue ellipticity (MRE) using the equation $[\Theta]_{MRE} = \Theta/(10ncl)$, where Θ is the ellipticity in millidegrees, n is the number of backbone peptide bonds (i.e., number of amino acid residues minus 1), c is the molar concentration of the sample, and l is the path length of the cuvette in centimeters. The melting temperature was determined by measuring a spectrum every 2 °C between 20 and 90 °C. The reaction buffer was incubated at each temperature for 5 min before the measurement of the spectrum. A blank run was always first performed using the buffer alone. Melting temperatures were extracted by fitting the data to an appropriate sigmoidal curve using the spectrometer software.

Steady-State Kinetic Measurements. Steady-state kinetic measurements were performed on a JASCO V-660 spectrophotometer. The steady-state rate constant (k_{cat}) was measured directly at saturating concentrations of NADPH (100 μM) and H_2F (100 μM). The enzyme activity was monitored spectrophotometrically at 340 nm [ε_{340}(cofactor + substrate) = 11800 M^{-1} cm^{-1}].[37] Rates were determined at pH 7 using 20−100 nM enzyme in 100 mM potassium phosphate containing 100 mM NaCl and 10 mM β-mercaptoethanol. The reaction buffer was preincubated at the desired temperature and the temperature in the cuvette monitored immediately prior to the acquisition of data. Initial linear rates of absorbance change were fit using the software provided by JASCO Corp. Each data point is the result of three independent measurements.

Pre-Steady-State Kinetic Measurements. Pre-steady-state kinetic experiments were performed on a Hi-Tech Scientific stopped-flow spectrophotometer. Hydride and deuteride transfer rate constants were measured following the transfer of fluorescence resonance energy from the protein to NADPH. Potassium phosphate buffer (100 mM, pH 7) containing 100 mM NaCl and 10 mM β-mercaptoethanol was used when the temperature was varied, and MTEN buffer (50 mM morpholinoethanesulfonic acid, 25 mM Tris, 25 mM ethanolamine, 100 mM NaCl, and 10 mM β-mercaptoethanol) was used when the pH was varied. The sample was excited at

dx.doi.org/10.1021/bi4005073 | *Biochemistry* 2013, 52, 3881−3887

297 nm and the emission measured using an output filter with a cutoff at 400 nm. NADPH(D) was preincubated with enzyme for 5 min at the desired temperature in a thermostated syringe compartment; the reaction was initiated by rapidly mixing this solution with H_2F. Final assay conditions were 20 μM enzyme, 8 μM NADPH(D), and 100 μM H_2F. The kinetic data were fit to a single-exponential decay.

RESULTS AND DISCUSSION

Design of an EcDHFR−TmDHFR Hybrid Enzyme. EcDHFR and TmDHFR have similar tertiary structures, and their N-terminal regions are highly conserved. However, residues in the M20 loop and the C-terminal region of EcDHFR, the corresponding regions of which form most of the dimer interface in TmDHFR,[25] are quite different from those found in TmDHFR[38] (Figure 1). The hydrophobic core of the dimer interface of TmDHFR consists mainly of aliphatic and aromatic residues, many of which are replaced with ionic and polar residues in EcDHFR (Figure 1). Hybrid enzymes of thermophilic and mesophilic alcohol dehydrogenases (ADH) have previously been created by exchanging the cofactor-binding domains involved in oligomerization.[39] However, when this approach was applied to the EcDHFR−TmDHFR pair, only misfolded aggregates were observed (see the Supporting Information). Hence, the stably folded EcDHFR−TmDHFR hybrid Xet-3 was generated by replacing 10 residues of EcDHFR with the corresponding amino acids that are directly involved in intersubunit interactions in TmDHFR (D11S and R12G in the M20 loop and H114V, D116P, E118V, S135L, S138M, S150G, C152L, and E154L in the C-terminal region) (Figure 1).

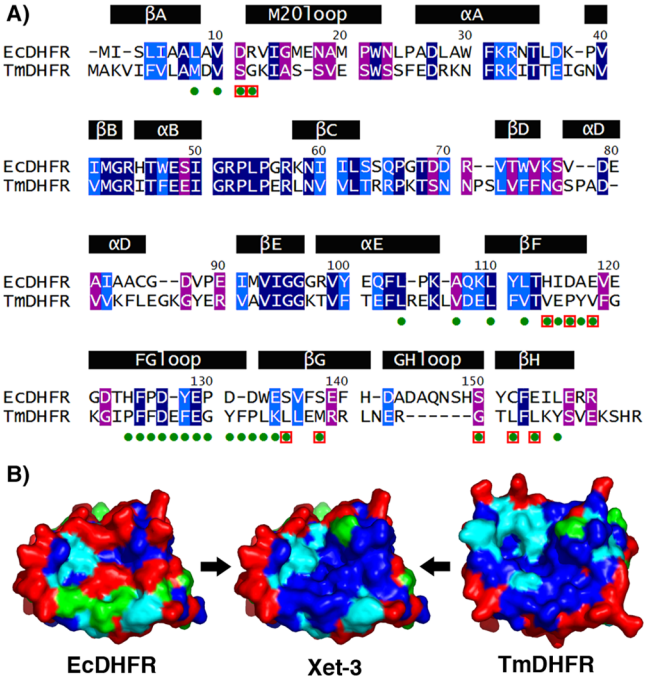

Figure 1. (A) Amino acid sequence alignment of EcDHFR and TmDHFR. Dark blue, light blue, and purple boxes indicate conserved, strongly similar, and weakly similar residues, respectively. Green dots below the sequence of TmDHFR indicate residues in the dimer interface. EcDHFR residues altered to the corresponding residues in TmDHFR to form Xet-3 are highlighted by red boxes below the sequence. (B) Surface representation (created with PyMol) of regions of TmDHFR involved in dimerization, and the corresponding regions of EcDHFR and Xet-3: red for charged residues, green for polar uncharged residues, blue for hydrophobic aliphatic residues, and cyan for aromatic residues.

Structural Analysis. To determine the oligomeric state of the recombinant protein under neutral conditions, EcDHFR, TmDHFR, and Xet-3 were subjected to size exclusion chromatographic analysis (Figure 2A). The elution profile of a 20 μM solution of Xet-3 shows two peaks at 10.0 and 12.5 mL. Monomeric EcDHFR and dimeric TmDHFR show only one peak with elution volumes of 12.2 and 10.2 mL, respectively, indicating that Xet-3 is a mixture of the monomer and dimer. The relative peak areas, moreover, change with the concentration of Xet-3, suggesting a slow equilibrium between these two states with an equilibrium constant of ~1 μM at 20 °C (Figure 2B). The Xet-3 dimer and monomer are relatively stable, as immediate re-injections of either isolated peak fraction onto the column give only a single peak (Figure 2A). The elution profiles remain unchanged after incubation at 4 °C for nearly 1 week. On the other hand, this equilibrium was re-established at elevated temperatures, with a half-life of ~5 h at 40 °C.

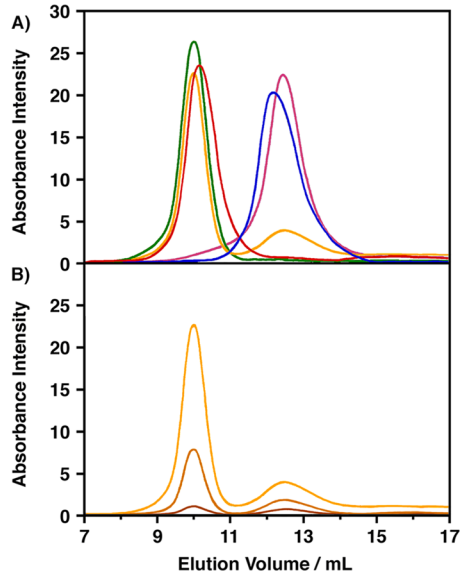

Figure 2. (A) Size exclusion chromatography of 20 μM Xet-3 (orange) and immediate re-injection of both peaks of Xet-3 (green and purple) in 100 mM potassium phosphate (pH 7) containing 100 mM NaCl at 20 °C. EcDHFR (blue) and TmDHFR (red) serve as monomer and dimer markers, respectively. (B) Size exclusion chromatography of Xet-3 at 20 (orange), 5 (dark orange), and 1 μM (brown) under the same conditions.

Far-UV CD spectra of the dimeric and monomeric fractions of Xet-3 were both characteristic of folded proteins (Figure 3A). There is a broad negative peak between 208 and 222 nm for both oligomeric states of Xet-3. The peak for the monomer is slightly wider and more intense than that of the dimer. At 20 °C, there is a minimal mean residue ellipticity (MRE) of −7485 deg cm^2 dmol^{-1} at 219 nm for the dimer and −6495 deg cm^2 dmol^{-1} at 222 nm for the monomer.

The thermal melting temperature (T_m) was measured by monitoring the change in MRE at 222 nm with an increasing temperature (Figure 3B). Thermal denaturation of both monomeric and dimeric forms of Xet-3 is not reversible

dx.doi.org/10.1021/bi4005073 | Biochemistry 2013, 52, 3881−3887

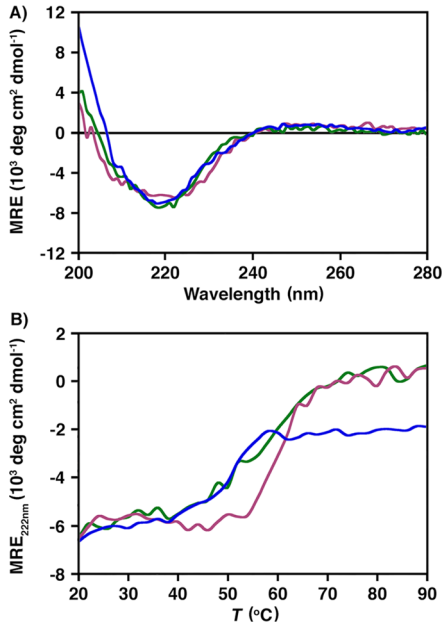

Figure 3. (A) CD spectra at 20 °C in 10 mM potassium phosphate buffer (pH 7) and (B) temperature dependence of the mean residue ellipticity at 222 nm of EcDHFR (blue), dimeric Xet-3 (green), and monomeric Xet-3 (purple).

because of the aggregation of the denatured proteins (not shown). Apparent T_m values were 57.2 ± 0.4 and 60.6 ± 0.3 °C for the monomeric and dimeric forms of Xet-3, respectively. Given the acceleration of the return to equilibrium at higher temperature (*vide supra*), it is likely that equilibrium is at least partly re-established during the measurement of T_m. The monomer/dimer ratio is probably therefore similar once higher temperatures are reached regardless of the starting populations. In any case, the T_m of Xet-3 is significantly higher than that of EcDHFR (51.2 ± 0.3 °C).[40]

Molecular modeling studies of EcDHFR and TmDHFR predict that the "hinge" region of EcDHFR around Asp87, far removed from the dimer interface of Xet-3, unfolds early in the denaturation process, while the β-sheet regions, which in TmDHFR are in the dimer interface, unfold relatively late.[27,40−42] Glycosylation at position 87 of EcDHFR is known to increase thermal stability,[43] whereas glycosylation on the βFG loop does not.[44] Therefore, the thermostability of Xet-3 may be limited by the unfolding of other regions of the enzyme that are afforded no additional protection by dimerization.

Steady-State Kinetics. The steady-state rate constants (k_{cat}) for the NADPH-dependent reduction of H_2F catalyzed by monomeric and dimeric Xet-3 at pH 7 increase in an exponential fashion up to 40 °C (Figure 4A and Table S1 of the Supporting Information) but decrease markedly at higher temperatures (data not shown). K_M values for the two forms are ∼4-fold higher than those of EcDHFR (Table 1), implying that the mutations have only a small effect on ligand binding. The affinity of Xet-3 for its ligands is more similar to that of EcDHFR than that of TmDHFR, as would be expected given that no active site mutations were introduced. In contrast, dimerization leads to a great decrease in the rate of turnover (Table 1). At 20 °C, the turnover number k_{cat} for the monomer of Xet-3 is 9-fold lower than that of EcDHFR, whereas the k_{cat} for the dimer of Xet-3 is almost 270-fold lower and comparable

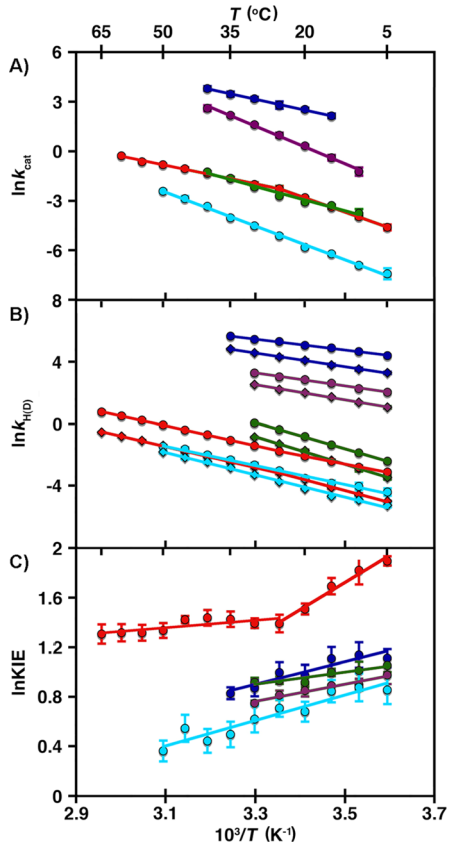

Figure 4. (A) Arrhenius plots of the steady-state rate constants, (B) Arrhenius plots for hydride (circles) and deuteride (diamond) transfer rate constants, and (C) corresponding KIEs on hydride transfer plotted on a logarithmic abscissa against the inverse temperature for EcDHFR (blue), the Xet-3 dimer (green), the Xet-3 monomer (purple), TmDHFR (red), and TmDHFR-V11D with CHAPS (cyan) at pH 7.

Table 1. k_{cat} and K_M Values at pH 7 and 20 °C for Catalysis by Wild-Type EcDHFR, TmDHFR, and Their Variants

enzyme	k_{cat} (s^{-1})	K_M^{NADPH} (μM)	$K_M^{H_2F}$ (μM)
EcDHFR	12.6 ± 1.4[19]	4.8 ± 1.0[35]	0.7 ± 0.3[35]
Xet-3 dimer	0.05 ± 0.01	19.9 ± 3.9	7.7 ± 1.4
Xet-3 monomer	1.39 ± 0.09	19.5 ± 3.5	2.7 ± 0.7
TmDHFR[26]	0.06 ± 0.01	<0.5	<0.5
TmDHFR-V11D with CHAPS[26]	0.003 ± 0.001	<1	<1

to that of TmDHFR. Monomerization of TmDHFR-V11D with CHAPS has previously been reported to lead to an ∼20-fold reduction in k_{cat}, whereas CHAPS had no effect on wild-type TmDHFR.[26]

Pre-Steady-State Kinetics. In a manner similar to the behavior of wild-type EcDHFR, the hydride transfer rate constants (k_H) at pH 7 for both oligomeric forms of Xet-3 (Figure 4B and Table S2 of the Supporting Information) are 5−30-fold higher than the k_{cat} values over the whole temperature range examined at neutral pH,[36] indicating that the chemical step is always a fast step in the catalytic cycle. As was seen for k_{cat}, dimerization causes a decrease in the k_H of Xet-3. At 20 °C, the k_H for the monomer (17.4 ± 0.6 s^{-1}) is 9-fold lower than that of wild-type EcDHFR (159.8 ± 7.9 s^{-1}),[32] whereas the k_H for the dimer is almost 400-fold lower (0.44 ±

dx.doi.org/10.1021/bi4005073 | *Biochemistry* 2013, 52, 3881−3887

0.02 s^{-1}) and is comparable to that of TmDHFR (0.122 ± 0.003 s^{-1}).[26] In contrast, monomerization of TmDHFR-V11D led to only a 4-fold reduction in k_H (0.029 ± 0.004 s^{-1}).

The primary KIE on hydride transfer was determined by replacing the cofactor NADPH with the deuterium-labeled alternative (NADPD) (Figure 4C and Tables S3−S5 of the Supporting Information). At 20 °C, the KIEs of the dimeric and monomeric Xet-3-catalyzed reactions are 2.50 ± 0.09 and 2.34 ± 0.12, respectively. Unlike TmDHFR-V11D, for which the temperature dependence of the KIE changes upon monomerization, it is not significantly affected by the quaternary structure of Xet-3. In addition, the dimeric form of Xet-3 does not show the breakpoint in the temperature dependence of the KIE observed for TmDHFR.[45] The breakpoint is not seen with other DHFRs, and its origin is not fully understood. However, mutations to the dimer interface of TmDHFR are known to remove the breakpoint and lead to monophasic KIEs.[24,26]

Xet-3 appears to also have active site electrostatic properties different from those of Ec- and TmDHFR. The apparent pK_a of the catalyzed reaction (Figure 5 and Table S6 of the Supporting Information) was found to be 7.48 ± 0.04 for monomeric Xet-3 and 8.05 ± 0.01 for dimeric Xet-3. In EcDHFR and TmDHFR, the apparent pK_a arises from protonation of N5 of the substrate dihydrofolate in the Michaelis complex,[19,46] and the same is likely to be true in Xet-3. Therefore, protonation of dihydrofolate appears to be more favorable in Xet-3 than in its parent enzymes; the apparent pK_a of the reaction catalyzed by EcDHFR is 6.48 ± 0.03,[47] while that of TmDHFR is 5.83 ± 0.06.[26] Protonation of H_2F may be favored in Xet-3 relative to EcDHFR because of a more tightly closed active site. This has been seen in computational studies of EcDHFR, where a "tightly closed" conformation of the Michaelis complex led to an increase to almost 9 of the pK_a of dihydrofolate.[48] The situation in TmDHFR is again different. Its active site is more open than that of EcDHFR;[25] hence, the pK_a is lower,[19,26] and monomerization does not decrease the pK_a.[26]

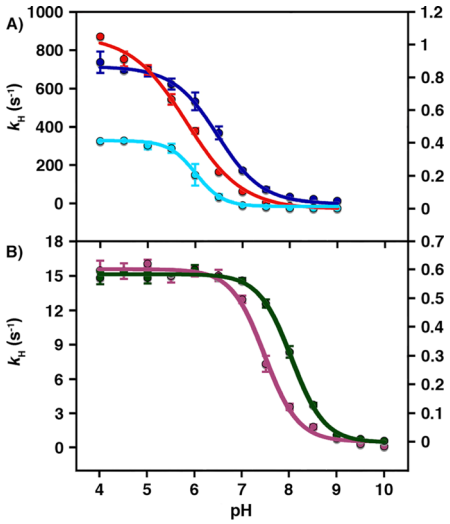

Figure 5. pH dependence of the hydride transfer rate constants for the reactions catalyzed by (A) EcDHFR (blue, left axis), TmDHFR (red, right axis), and TmDHFR-V11D (cyan, right axis) and (B) Xet-3 in its monomeric (purple, left axis) and dimeric (green, right axis) forms.

CONCLUSIONS

The results presented here show that the effects of subunit interactions on catalysis are totally different in Xet-3 and TmDHFR. Dimerization in Xet-3 makes protonation of the substrate more favorable and reduces the rate constants for both hydride transfer and overall catalytic turnover. It has no effect on the temperature dependence of the observed kinetic isotope effects on hydride transfer. In TmDHFR-V11D, monomerization reduces the rate constant for overall turnover and changes the temperature dependence of the observed kinetic isotope effects on hydride transfer but has no significant effect on the rate constants for hydride transfer or the protonation state of the substrate. Because Xet-3 originates predominantly from EcDHFR, the data presented here demonstrate that the catalytic cycles of EcDHFR and TmDHFR, and the roles of their respective loop regions, are markedly different. Release of the constrained loops around the interface region in TmDHFR does not simply have the opposite effect of applying such a constraint in EcDHFR. Dimerization of EcDHFR likely restrains or otherwise alters the behavior of the M20, βFG, and GH loops, which are crucial in adopting the correct conformations for efficient progression through the catalytic cycle,[49] and therefore decreases the rate of catalytic turnover. As conformational motions do not drive the chemical step of DHFR catalysis through barrier narrowing,[24,33,47,50,51] the decrease in the hydride transfer rate constant upon dimerization of Xet-3 is likely due to subtle changes to the geometry and electrostatics of the active site, although these changes also facilitate the favorable protonation of the substrate. In contrast, the loss of intersubunit interactions in TmDHFR and the likely increase in the flexibility of the loop regions normally involved in dimerization are detrimental to catalytic turnover but not to hydride transfer. Because *T. maritima* has a ThyX-type thymidylate synthase,[52] which regenerates tetrahydrofolate rather than oxidizing it to dihydrofolate, and because tetrahydrofolate is particularly unstable at higher temperatures, only very low DHFR activity is required.[32] The predominant evolutionary pressure on TmDHFR is therefore for thermostability rather than for rapid turnover of the substrate. Lastly, while the positive effect of oligomerization on the thermostability of enzymes has been well documented,[53,54] its effect on catalysis greatly depends on the interactions between the oligomer interface and the active site. In a similar study of tetrameric ADH from *T. brockii*, monomerization upon engineering results in no detectable enzyme activity because part of the active site is located at the interface between subunits.[39] Conversely, there is essentially no effect on activity when phosphoribosylanthranilate isomerase from *T. maritima* is monomerized, because the dimer interface is fairly distant from the active site.[55]

In summary, EcDHFR has been dimerized by mimicking the interface region of TmDHFR. The resulting EcDHFR−TmDHFR hybrid, Xet-3, exists as a mixture of the dimer and monomer, which interconvert only slowly even at elevated temperatures. CD spectroscopy shows that the dimeric and monomeric forms of Xet-3 shared similar secondary structure with EcDHFR. The apparent T_m of Xet-3 is ∼6−9 °C higher than that of wild-type EcDHFR, demonstrating some protection from thermal denaturation. Monomerization of TmDHFR (as in TmDHFR-V11D) leads to an ∼20 °C decrease in the T_m.[26] Additional changes to EcDHFR are

dx.doi.org/10.1021/bi4005073 | *Biochemistry* 2013, 52, 3881−3887

therefore required to attain a thermostability similar to that of TmDHFR.

The monomeric form of Xet-3 shows steady-state and pre-steady-state rate constants similar to those of wild-type EcDHFR. However, both kinetic parameters of the dimeric form are much lower than those of the monomeric form and are highly similar to the corresponding values for TmDHFR. In the case of the monomeric TmDHFR-V11D, k_H remains similar to that of the dimeric wild-type counterpart but k_{cat} is reduced dramatically. The results presented here demonstrate that the effect of dimerization and/or monomerization on catalysis is significantly different for EcDHFR and TmDHFR. In EcDHFR, the physical steps of the catalytic cycle are promoted by movement of flexible loop regions, so restricting their movement in Xet-3 leads to lower values of k_{cat}. k_H is also reduced, most likely because of subtle structural changes that propagate to the active site.[40] In TmDHFR, on the other hand, monomerization is detrimental to catalysis, demonstrating that loop flexibility is not an important factor in TmDHFR catalysis.

This work demonstrates that TmDHFR cannot simply be considered in the same way as monomeric DHFRs. Possibly as a result of differing selective pressures on TmDHFR compared to those of monomeric DHFRs, the effect of monomerization on TmDHFR catalysis is very different from that predicted via EcDHFR catalysis. Interpreting the effects of oligomerization on the catalytic efficiency of thermophilic enzymes in terms of their mesophilic counterparts is therefore not appropriate. Broad conclusions of the effect of oligomerization on the catalytic efficiency of thermophilic enzymes in general are therefore difficult. Our results therefore suggest that while EcDHFR may serve as a paradigmatic system for the study of enzyme catalysis in general, it is not a good model for the details of catalysis by other DHFRs.

■ ASSOCIATED CONTENT

Supporting Information

Details of failed attempts to create EcDHFR−TmDHFR hybrid enzymes and tables of kinetic data. This material is available free of charge via the Internet at http://pubs.acs.org.

■ AUTHOR INFORMATION

Corresponding Author

*School of Chemistry and Cardiff Catalysis Institute, Cardiff University, Main Building, Park Place, Cardiff CF10 3AT, United Kingdom. E-mail: allemannrk@cf.ac.uk. Phone: (44) 29 2087 9014. Fax: (44) 29 2087 4030.

Funding

This work was supported by Grant BB/J005266/1 (R.K.A.) from the UK Biotechnology and Biological Sciences Research Council and by the Vice Chancellor Fund of Cardiff University.

Notes

The authors declare no competing financial interest.

■ ABBREVIATIONS

CD, circular dichroism; CHAPS, 3-[(3-cholamidopropyl)-dimethylammonio]-1-propanesulfonate; DHFR, dihydrofolate reductase; EcDHFR, DHFR from *E. coli*; H_2F, 7,8-dihydofolate; H_4F, 5,6,7,8-tetrahydrofolate; KIE, kinetic isotope effect; MRE, mean residue ellipticity; $NADP^+$, nicotinamide adenine dinucleotide phosphate; NADPH, reduced nicotinamide adenine dinucleotide phosphate; OD, optical density; TmDHFR, DHFR from *T. maritima*.

■ REFERENCES

(1) Bergey, D. H. (1919) Thermophilic bacteria. *J. Bacteriol. 4*, 301−306.

(2) Haney, P., Konisky, J., Koretke, K. K., Luthey-Schulten, Z., and Wolynes, P. G. (1997) Structural basis for thermostability and identification of potential active site residues for adenylate kinases from the archaeal genus *Methanococcus*. *Proteins 28*, 117−130.

(3) Russell, R. J. M., Ferguson, J. M. C., Hough, D. W., Danson, M. J., and Taylor, G. L. (1997) The crystal structure of citrate synthase from the hyperthermophilic *Archaeon pyrococcus* furiosus at 1.9 Å resolution. *Biochemistry 36*, 9983−9994.

(4) Watanabe, K., Hata, Y., Kizaki, H., Katsube, Y., and Suzuki, Y. (1997) The refined crystal structure of *Bacillus cereus* oligo-1,6-glucosidase at 2.0 Å resolution: Structural characterization of proline-substitution sites for protein thermostabilization. *J. Mol. Biol. 269*, 142−153.

(5) Bogin, O., Peretz, M., Hacham, Y., Korkhin, Y., Frolow, F., Kalb, A. J., and Burstein, Y. (1998) Enhanced thermal stability of *Clostridium beijerinckii* alcohol dehydrogenase after strategic substitution of amino acid residues with prolines from the homologous thermophilic *Thermoanaerobacter brockii* alcohol dehydrogenase. *Protein Sci. 7*, 1156−1163.

(6) Vogt, G., and Argos, P. (1997) Protein thermal stability: Hydrogen bonds or internal packing? *Folding Des. 2*, S40−S46.

(7) Vogt, G., Woell, S., and Argos, P. (1997) Protein thermal stability, hydrogen bonds, and ion pairs. *J. Mol. Biol. 269*, 631−643.

(8) Salminen, T., Teplyakov, A., Kankare, J., Cooperman, B. S., Lahti, R., and Goldman, A. (1996) An unusual route to thermostability disclosed by the comparison of *Thermus thermophilus* and *Escherichia coli* inorganic prophosphatases. *Protein Sci. 5*, 1014−1025.

(9) Synowiecki, J. (2010) Some applications of thermophilies and their enzymes for protein processing. *Afr. J. Biotechnol. 9*, 7020−7025.

(10) Oyeyemi, O. A., Sours, K. M., Lee, T., Resing, K. A., Ahn, N. G., and Klinman, J. P. (2010) Temperature denpendence of protein motions in a thermophilic dihydrofolate reductase and its relationship to catalytic efficiency. *Proc. Natl. Acad. Sci. U.S.A. 107*, 10074−10079.

(11) Bhabha, G., Lee, J., Ekiert, D. C., Gam, J., Wilson, I. A., Dyson, H. J., Benkovic, S. J., and Wright, P. E. (2011) A dynamic knockout reveals that conformational fluctuation influence the chemical step of enzyme catalysis. *Science 332*, 234−238.

(12) Adamczyk, A. J., Cao, J., Kamerlin, S. C. L., and Warshel, A. (2011) Catalysis by dihydrofolate reductase and other enzymes arises from electrostatic preorganization, not conformational motions. *Proc. Natl. Acad. Sci. U.S.A. 108*, 14115−14120.

(13) Georlette, D., Damien, B., Blaise, V., Depiereux, E., Uversky, V. N., Gerday, C., and Feller, G. (2003) Structural and functional adaptations to extreme temperatures in psychrophilic, mesophilic, and thermophilic DNA ligases. *J. Biol. Chem. 278*, 37015−37023.

(14) Bae, E., and Phillips, G. N. (2004) Structures and analysis of highly homologous psychrophilic, and thermophilic adenylate kinases. *J. Biol. Chem. 279*, 28202−28208.

(15) Zavodszky, P., Kardos, J., Svingor, A., and Petsko, G. A. (1998) Adjustment of conformational flexibility is a key event in the thermal adaptation of proteins. *Proc. Natl. Acad. Sci. U.S.A. 95*, 7406−7411.

(16) Charlton, P. A., Young, D. W., Birdsall, B., Feeney, J., and Roberts, G. C. K. (1979) Stereochemistry of reduction of folic-acid using dihydrofolate-reductase. *J. Chem. Soc., Chem. Commun.*, 922−924.

(17) Charlton, P. A., Young, D. W., Birdsall, B., Feeney, J., and Roberts, G. C. K. (1985) Stereochemistry of reduction of the vitamin folic-acid by dihydrofolate-reductase. *J. Chem. Soc., Perkin Trans. 1*, 1349−1353.

(18) Stojković, V., Perissinotti, L. L., Lee, J., Benkovic, S. J., and Kohen, A. (2010) The effect of active-site isoleucine to alanine mutation on the DHFR catalyzed H-transfer. *Chem. Commun. 46*, 8974−8976.

(19) Maglia, G., Javed, M. H., and Allemann, R. K. (2003) Hydride transfer during catalysis by dihydrofolate reductase from *Thermotoga maritima*. *Biochem. J. 374*, 529−535.

(20) Dams, T., Bohm, G., Auerbach, G., Bader, G., Schuring, H., and Jaenicke, R. (1998) Homo-dimeric recombinant dihydrofolate reductase from *Thermotoga maritima* shows extreme intrinsic stability. *Biol. Chem. 379*, 367−371.
(21) Dams, T., and Jaenicke, R. (1999) Stability and folding of dihydrofolate reductase from the hyperthermophilic bacterium *Thermotoga maritima*. *Biochemistry 38*, 9169−9178.
(22) Wilquet, V., Gaspar, J. A., van de Lande, M., van de Casteele, M., Legrain, C., Meiering, E. M., and Glansdorff, N. (1998) Purification and characterization of recombinant *Thermotoga maritima* dihydrofolate reductase. *Eur. J. Biochem. 255*, 628−637.
(23) Pijning, T., van Pouderoyen, G., Kluskens, L., van der Oost, J., and Dijkstra, B. W. (2009) The crystal structure of a hyperthermoactive exopolygalacturonase from *Thermotoga maritima* reveals a unique tetramer. *FEBS Lett. 583*, 3665−3670.
(24) Loveridge, E. J., and Allemann, R. K. (2010) The temperature dependence of the kinetic isotope effects of dihydrofolate reductase from *Thermotoga maritima* is influenced by intersubunit interactions. *Biochemistry 49*, 5390−5396.
(25) Dams, T., Auerbach, G., Bader, G., Jacob, U., Ploom, T., Huber, R., and Jaenicke, R. (2000) The crystal structure of dihydrofolate reductase from *Thermotoga maritima*: Molecular features of thermostability. *J. Mol. Biol. 297*, 659−672.
(26) Loveridge, E. J., Rodriguez, R. J., Swanwick, R. S., and Allemann, R. K. (2009) Effect of dimerization on the stability and catalytic activity of dihydrofolate reductase from the hyperthermophile *Thermotoga maritima*. *Biochemistry 48*, 5922−5933.
(27) Pang, J. Y., and Allemann, R. K. (2007) Molecular dynamics simulation of thermal unfolding of *Thermatoga maritima* DHFR. *Phys. Chem. Chem. Phys. 9*, 711−718.
(28) Radkiewicz, J. L., and Brooks, C. L. (2000) Protein dynamics in enzymatic catalysis: Exploration of dihydrofolate reductase. *J. Am. Chem. Soc. 122*, 225−231.
(29) Agarwal, F. K., Billeter, S. R., Rajagopalan, P. T. R., Benkovic, S. J., and Hammes-Schiffer, S. (2002) Network of coupled promoting motions in enzyme catalysis. *Proc. Natl. Acad. Sci. U.S.A. 99*, 2794−2799.
(30) Benkovic, S. J., and Hammes-Schiffer, S. (2003) A perspective on enzyme catalysis. *Science 301*, 1196−1202.
(31) Pang, J. Y., Pu, J. Z., Gao, J. L., Truhlar, D. G., and Allemann, R. K. (2006) Hydride transfer reaction catalyzed by hyperthermophilic dihydrofolate reductase is dominated by quantum mechanical tunneling and is promoted by both inter- and intramonomeric correlated motions. *J. Am. Chem. Soc. 128*, 8015−8023.
(32) Loveridge, E. J., Maglia, G., and Allemann, R. K. (2009) The role of arginine 28 in catalysis by dihydrofolate reductase from the hyperthermophile *Thermotoga maritima*. *ChemBioChem 10*, 2624−2627.
(33) Loveridge, E. J., and Allemann, R. K. (2011) Effect of pH on hydride transfer by *Escherichia coli* dihydrofolate reductase. *ChemBioChem 12*, 1258−1262.
(34) Zakrzewski, S. F. (1966) On mechanism of chemical and enzymatic reduction of folate and dihydrofolate. *J. Biol. Chem. 241*, 2962−2967.
(35) Fierke, C. A., Johnson, K. A., and Benkovic, S. J. (1987) Construction and evaluation of the kinetic scheme associated with dihydrofolate reductase from *Escherichia coli*. *Biochemistry 26*, 4085−4092.
(36) Swanwick, R. S., Maglia, G., Tey, L.-H., and Allemann, R. K. (2006) Coupling of protein motions and hydrogen transfer during catalysis by *Escherichia coli* dihydrofolate reductase. *Biochem. J. 394*, 259−265.
(37) Stone, S. R., and Morrison, J. F. (1982) Kinetic mechanism of the reaction catalyzed by dihydrofolate reductase from *Escherichia coli*. *Biochemistry 21*, 3757−3765.
(38) Bolin, J. T., Filman, D. J., Matthews, D. A., Hamlin, R. C., and Kraut, J. (1982) Crystal-structures of *Escherichia coli* and *Lactobacillus casei* dihydrofolate-reductase refined at 1.7 Å resolution. 1. General features and binding of methotrexate. *J. Biol. Chem. 257*, 3650−3662.
(39) Goihberg, E., Peretz, M., Tel-Or, S., Dym, O., Shimon, L., Frolow, F., and Burstein, Y. (2010) Biochemical and structural properties of chimeras constructed by exchange of cofactor-binding domains in alcohol dehydrogenases from thermophilic and mesophilic microorganisms. *Biochemistry 49*, 1943−1953.
(40) Swanwick, R. S., Shrimpton, P. J., and Allemann, R. K. (2004) Pivotal role of Gly 121 in dihydrofolate reductase from *Escherichia coli*: The altered structure of a mutant enzyme may form the basis of its diminished catalytic performance. *Biochemistry 43*, 4119−4127.
(41) Sham, Y. Y., Ma, B. Y., Tsai, C. J., and Nussinov, R. (2002) Thermal unfolding molecular dynamics simulation of *Escherichia coli* dihydrofolate reductase: Thermal stability of protein domains and unfolding pathway. *Proteins 46*, 308−320.
(42) Frieden, C. (1990) Refolding of *Escherichia coli* dihydrofolate reductase: Sequential formation of substrate binding sites. *Proc. Natl. Acad. Sci. U.S.A. 87*, 4413−4416.
(43) Swanwick, R. S., Daines, A. M., Tey, L. H., Flitsch, S. L., and Allemann, R. K. (2005) Incresed thermal stability of site-selectively glycosylated dihydrofolate reductase. *ChemBioChem 6*, 1338−1340.
(44) Tey, L. H., Loveridge, E. J., Swanwick, R. S., Flitsch, S. L., and Allemann, R. K. (2010) Highly site-selective stability increases by glycosylation of dihydrofolate reductase. *FEBS J. 277*, 2171−2179.
(45) Maglia, G., and Allemann, R. K. (2003) Evidence for environmentally coupled hydrogen tunneling during dihydrofolate reductase catalysis. *J. Am. Chem. Soc. 125*, 13372−13373.
(46) Chen, Y.-Q., Kraut, J., Blakely, R. L., and Callender, R. (1994) Determination by raman spectroscopy of the pKa of N5 of dihydrofolate bond to dihydrofolate reductase: Mechanistic implications. *Biochemistry 33*, 7021−7026.
(47) Loveridge, E. J., Tey, L.-H., and Allemann, R. K. (2010) Solvent effects on catalysis by *Escherichia coli* dihydrofolate reductase. *J. Am. Chem. Soc. 132*, 1137−1143.
(48) Khavrutskii, I. V., Price, D. J., Lee, J., and Brooks, C. L. (2007) Comformational change of the methionine 20 loop of *Escherichia coli* dihydrofolate reductase modulates pK_a of the bound dihydrofolate. *Protein Sci. 16*, 1087−1100.
(49) Sawaya, M. R., and Kraut, J. (1997) Loop and subdomain movements in the mechanism of *Escherichia coli* dihydrofolate reductase: Crystallographic evidence. *Biochemistry 36*, 586−603.
(50) Loveridge, E. J., Tey, L.-H., Behiry, E. M., Dawson, W. M., Evans, R. M., Whittaker, S. B.-M., Gunther, U. L., Williams, C., Crump, M. P., and Allemann, R. K. (2011) The role of large-scale motion in catalysis by dihydrofolate reductase. *J. Am. Chem. Soc. 133*, 20561−20570.
(51) Loveridge, E. J., Behiry, E. M., Guo, J., and Allemann, R. K. (2012) Evidence that a 'dynamic knockout' in *Escherichia coli* dihydrofolate reductase does not affect the chemical step of catalysis. *Nat. Chem. 4*, 292−297.
(52) Kuhn, P., Lesley, S. A., Mathews, I. I., Canaves, J. M., Brinen, L. S., Dai, X. P., Deacon, A. M., Elsliger, M. A., Eshaghi, S., Floyd, R., Godzik, A., Grittini, C., Klock, H. E., Koesema, E., Kovarik, J. M., Kreusch, A. T., McMullan, D., McPhillips, T. M., Miller, M. A., Miller, M., Morse, A., Moy, K., Ouyang, J., Robb, A., Rodrigues, K., Selby, T. L., Spraggon, G., Stevens, R. C., Taylor, S. S., van der Bedem, H., Velasquez, J., Vincnet, J., Wang, X. H., West, B., Wolf, G., Wooley, J., and Wilson, I. A. (2002) Crystal structure of Thy1, a thymidylate synthase complementing protein from *Thermotoga maritima* at 2.25 Å resolution. *Proteins 49*, 142−145.
(53) Tanaka, Y., Tsumoto, K., Yasutake, Y., Umetsu, M., Yao, M., Fukada, H., Tanaka, I., and Kumaga, I. (2004) How oligomerization contributes to the thermostability of an archaeon protein. *J. Biol. Chem. 279*, 32957−32967.
(54) Gerk, L. P., Levon, O., and Muller-Hill, B. (2000) Strengthening the dimerisation interface of Lac repressor increases its thermostability by 40 °C. *J. Mol. Biol. 299*, 805−812.
(55) Thoma, R., Hennig, M., Sterner, R., and Kirschner, K. (2000) Structure and function of mutationally generated monomers of dimeric phosphoribosylanthranilate isomerase from *Thermotoga maritima*. *Structure 8*, 265−276.